Published OnlineFirst February 2, 2015; DOI: 10.1158/1535-7163.MCT-14-0862

enzyme inhibitors ineffective, and second-generation therapies are designed based upon the specific evasion mechanisms observed in patient tumors (10, 11). For antibody-targeted therapies, multiple mechanisms are emerging which may mediate drug treatment failure. Resistance to the anti-Her2 antibody, trastuzumab, is reportedly associated with receptor shedding, signaling pathway activation, including PIK3CA mutation, PTEN loss, elevated Rac1 GTPase activity, or induction of other receptors; i.e., IGF1R and Her3; refs. 12, 13). Resistance to anti-VEGF antibody, bevacizumab, may also be regulated by induction of alternate angiogenic signaling pathways (14).

There are limited data on the acquisition of resistance to ADCs as these biotherapeutics are relative newcomers to the clinic and patient data are still emerging. One experimental model of ADC resistance was generated by serial exposure of a lung adenocarcinoma xenograft in athymic mice to *Vinca*-conjugated anti-KS1/4 ADC, and no ABCB1 (MDR1) drug transporter mRNA or protein were observed (15). Tumors inherently refractory to the clinically approved ADC, T-DM1, are reported in both preclinical and clinical settings, although mechanisms of resistance have not been elucidated (16). Phillips and colleagues (17) reported induction of resistance in cultured breast carcinoma cell lines by stepwise exposure to T-DM1. Increased MDR1 and reduced Her2 were observed in KPL4 cells, but not in BT474M1, suggesting that different cell lineages may become refractory to the same ADC via divergent mechanisms. Recently, Phillips and colleagues (18) reported that heregulin (NRG1β) attenuates the response of several Her2-expressing cell lines to T-DM1, as well as to other microtubule inhibitors. Lewis and colleagues (19) recently created three cultured lymphoma cell lines with >1,000-fold acquired resistance to brentuximab vedotin (anti-CD30-mcValCitPABC-MMAE), and observed mixed phenotypes of MDR1 induction and/or loss of CD30 antigen among the models.

In the current study, an anti-Her2 trastuzumab–maytansinoid antibody–drug conjugate (TM-ADC), which is structurally similar to T-DM1, was used to generate cells resistant to the ADC *in vitro*. These data suggest that it may be possible to treat TM-ADC–refractory cancer cells via a cassette-based approach of switching the linker of immunoconjugates, or to treat with unconjugated standard chemotherapeutics of similar inhibitor class as the targeted payload.

Materials and Methods

Cell lines

JIMT1 cells were obtained from DSMZ, and were originally established from the pleural metastasis of a patient with breast carcinoma who had failed trastuzumab therapy (20). MDA-MB-361-DYT2 cells are derived from metastatic breast carcinoma and were generously provided by Dr. Dajun Yang at Georgetown University (Washington D.C.) Cell line authentication was conducted in May 2014 by short tandem repeat analysis (Idexx BioResearch) and confirmed that all four cell lines (both parental and resistant models) are of human origin and that the 16 genetic profile markers evaluated in the panel are identical to those previously reported for the respective parental cell line. JIMT1 cells were maintained in DMEM supplemented with 10% FBS, 1% L-glutamine, and 1% sodium pyruvate. MDA-MB-361-DYT2 cells were maintained in MEM supplemented with 10% FBS, 1% L-glutamine, 1% sodium pyruvate, 1% nonessential amino acids, and 2% MEM vitamins. H69 and H69AR cell lines were obtained from ATCC and were maintained in RPMI/25 mmol/L HEPES media supplemented with 10% FBS, 1% L-glutamine, 1% sodium pyruvate. KB, KB-8.5, and KB-V1 cells were generously provided by Dr. Michael Gottesman, NCI (Bethesda, MD), and were maintained in DMEM supplemented with 10% FBS, 1% sodium pyruvate, and 1% L-glutamine.

Bioconjugations

Trastuzumab–maytansinoid conjugate (TM-ADC) is structurally similar to trastuzumab emtansine (T-DM1, or Kadcyla), and is comprised of anti-Her2 trastuzumab antibody covalently bound to DM1 through a bifunctional linker. Conjugation was conducted as described previously (21), and all ADC preparations are detailed in Supplementary Materials and Methods.

Procedure to make cell lines resistant to TM conjugate

Cells were exposed to multiple cycles of TM conjugate at approximately IC_{80} concentrations for 3 days, followed by approximately 4 to 11 days recovery without treatment. The procedure was intended to simulate the chronic, multicycle (on/off) dosing at maximally tolerated doses typically used for cytotoxic therapeutics in the clinic, followed by a recovery period (Supplementary Fig. S1). Parental cells derived from MDA-MB-361-DYT2 are referred to as 361, and cells chronically exposed to TM-ADC are referred to as 361-TM. JIMT1 cells chronically exposed to TM-ADC are referred to as JIMT1-TM. Further details can be found in Supplementary Materials and Methods.

Cytotoxicity assay

Cells were seeded in 96-well plates at low density, then treated the following day with ADCs or unconjugated payloads at 3-fold serial dilutions at 10 concentrations in duplicate. Cells were incubated for 4 days in a humidified 37°C/5% CO_2 incubator. Plates were incubated with CellTiter 96 AQueous One MTS Solution (Promega) for 1 hour and absorbance measured on a Victor plate reader (Perkin-Elmer) at 490 nm. IC_{50} values were calculated using a four-parameter logistic model with XLfit (IDBS). For studies using ABCC1 reversal agent, reversan (Millipore), was added to either 1 or 6 μmol/L final concentrations in combination with ADC treatment. No cytotoxicity was observed after 4 days with reversan alone at doses up to 10 μmol/L.

In vivo efficacy studies

All animal studies were approved by the Pfizer Pearl River Institutional Animal Care and Use Committee according to established guidelines. Female NOD *scid* gamma (NSG) immunodeficient mice (NOD.Cg-Prkdc^{scid} Il2rg^{tm1Wjl}/SzJ) were obtained from The Jackson Laboratory. Mice were injected subcutaneously in the right flank with suspensions of either 361 or 361-TM cells in 50% Matrigel (1×10^6 cells per injection). Mice were randomized into study groups when tumors reached approximately 0.3 g. TM-ADC conjugate (3 mg/kg) or vehicle were administered intravenously in saline on day 0 and repeated for a total of four doses, 4 days apart. Tumors were measured weekly and mass calculated as volume = (width × width × length)/2. Time-to-event analysis (tumor doubling) was conducted and significance evaluated by log-rank (Mantel–Cox) test. No weight loss was observed in mice in all treatment groups in these studies.

Published OnlineFirst February 2, 2015; DOI: 10.1158/1535-7163.MCT-14-0862

Immunoblot analyses

Whole-cell lysates were prepared in TBS with 1% Igepal, 0.25% sodium deoxycholate, supplemented with protease inhibitor cocktail (Sigma). Samples were fractioned and analyzed by immunoblot. Cell surface protein extracts were prepared as described in "Proteomic Profiling" methods section below. Whole-cell lysates or cell surface enriched samples were fractionated on 4%–20% SDS-PAGE, transferred to polyvinylidene difluoride membranes, and probed with the indicated antibodies to the following antigens: Her2 (Cell Signaling Technology; cat# 2248), ABCC1/MRP1 (Enzo Life Science; cat# ALX-801-007), ABCB1/MDR1 (OriGene; cat# TA801056), actin (Millipore; cat# MAB1501R), RABGAP1 (Abcam; cat# ab107330), PAK4 (Abcam; cat# ab62509), and HECTD1(Abcam; cat# ab101992). Secondary antibodies used were horseradish peroxidase (HRP)-conjugated goat anti-mouse IgG (Bio-Rad; cat# 170-6520), HRP-conjugated goat anti-rabbit IgG (Bio-Rad, cat# 170-6518), HRP-conjugated goat anti-rat IgG (Enzo Life Sciences, cat# ADI-SAB-220).

Antibody-binding studies

Trastuzumab binding to the cell surface was evaluated by indirect immunofluorescence staining and flow cytometry. Cells (2×10^5/well) were incubated with antibody at various concentrations for 1 hour on ice, followed by washing with PBS, then incubated with phycoerythrin (PE)-conjugated goat anti human IgG (Cat#109-116-098, Jackson ImmunoResearch) for 30 minutes on ice. After washing thoroughly with PBS, cells were analyzed by flow cytometry with an Accuri system (BD Biosciences). For ABCC1 (MRP1) antibody binding, cells were trypsinized, washed twice with cold PBS, fixed with 1% paraformaldehyde in PBS for 30 minutes at 4°C, then washed once with cold blocking solution (1% BSA/PBS). After fixing, cells were incubated in cold cell permeabilization buffer (CPB: 1% BSA/0.1% Tween-20/PBS) for 30 minutes at 4°C. Cells (2×10^5/well) were incubated with mouse anti-MRP1 monoclonal antibody (Cat# MAB4100, Millipore) in CPB at various concentrations for 1 hour on ice, followed by washing with CPB, then incubated with PE-conjugated goat anti-mouse IgG (Cat# 115-115-164, Jackson ImmunoResearch) in CPB for 30 minutes on ice. After washing thoroughly, cells were resuspended in 1% paraformaldehyde/PBS buffer and analyzed by flow cytometry (Accuri).

Rhodamine-123 accumulation assay

Cells (2×10^5 cells/mL) were preloaded with rhodamine-123 (Millipore) for 2 hours on ice, then washed thoroughly with efflux buffer (RPMI1640 with 3% BSA). Cells were resuspended in warm efflux buffer with or without 20 μmol/L reversan (Millipore), incubated for 2 hours at 37°C in the dark, washed, and analyzed by flow cytometry to measure Rhodamine-123 retention.

Proteomic profiling and analyses

Subconfluent cells were detached with CellStripper (Mediatech) and washed with PBS. Approximately $0.5–1 \times 10^7$ cells were labeled with 1.5 mmol/L NHS-β-Ala-Asp3-biotin solution for 1 hour at 4°C in the dark. After labeling, cells were washed, lysed, and 1,000 μg total protein was incubated with 50 μL of packed neutravidin resin for 2 hours at 4°C in the dark to capture cell surface–associated proteins. Protein–resin complexes were washed, then dissociated by boiling in 40 μL 2× SDS sample buffer for 5 minutes. Captured cell surface proteins were fractionated on-gel, processed into eight fractions, each reduced with dithiothreitol, alkylated with idoacetamine, and digested with trypsin. Resulting peptides were fractionated by nano-LC using a custom fabricated C18 column, and detected by nano-electrospray ionization on Thermo LTQ Orbitrap Velos operating at 60,000 resolution over a mass range of 300–2000 Da in parallel scanning mode with dynamic exclusion, where the top 20 most intense ions were selected for tandem mass spectrometry fragmentation in the ion trap. Resulting raw spectra were converted to mzXML and spectra were matched to peptides in a modified version of the Human IPI database v3.84 (90166 entries) by the MyriMatch MVH algorithm using default settings with the following exceptions: precursor tolerance was set to 10 ppm, fragment tolerance was set to 0.5 Da, semitryptic cleavage rules were used, and alkylated cysteines and oxidized methionine were defined as dynamic modifications (MyriMatch). A parsimonious protein summary was compiled using IDPicker with peptide inclusion set at 5% false discovery rate and protein inclusion requiring 2 unique peptides. Spectral count data were updated, so that 0 values were replaced by 0.5, normalized by column sum spectral count and scaled by the average columns sum spectral count for all groups, and these values were scaled by a constant (10,000) and represent relative protein abundance. Data were then $\log_2$ transformed and analyzed using Statistical Analysis of Microarrays (SAM) implemented in R (22). Differential expression was evaluated for each protein by fold change and statistical significance when comparing parental and resistant replicate samples. Significant proteins in resistant cell profiles with differential expression with 2-fold difference from parental were summarized by gene equivalents and were searched for gene set enrichmet using Pathway Commons Analysis in the WEB-based GEne SeT AnaLysis Toolkit (WebGestalt) by comparing against the *hspiens__entrezgene_protein_coding* reference set for Enrichment Analysis with default statistical methods (hypergeometric with BH multiple test adjustment), significance level (top 10), and minimum number of gene category of 2; all gene sets available in WebGestalt are previously described (23). Pathway databases used are KEGG (March 21, 2011) and Pathway Commons (November 11, 2012). For some analyses, proteomic data were filtered directly with gene sets representing the endosome (GO: 005768) and lysosome (GO: 0005764) gene ontology obtained from the GO Consortium.

Transcriptional profiling

Total RNA was extracted from individual cell cultures in triplicate by resuspending cells in 0.6 mL RLT lysis buffer, purified with RNeasy Kit (Qiagen), and labeled using Genechip 3′ IVT express kit (Affymetrix) following the manufacturer's protocols. Each biotin labeled RNA sample (2 μg) was hybridized to HgU133_+2.0 oligonucleotide arrays (Affymetrix) and subsequently washed, stained, and scanned on Affymetrix 3000 Genechip Scanner. Affymetrix MAS5.0 software was used to convert raw fluorescence data into mRNA signal intensity and present/absent absolute calls. Only probe sets called present in all three samples of at least one cohort with a minimum mean signal intensity of 50 were used in the analysis. Data analysis was based on a combination of fold-change in comparison of mean signal intensity values and *t* test of statistical significance. Gene data for ABCC1: ID = 4363, Gene = ABCC1, Description = 202804_at ATP-binding cassette, subfamily C (CFTR/MRP), member 1. Gene data for ERBB2: ID = 2064, Gene = ERBB2; Description = 216836_s_at v-erb-b2 erythroblastic

Published OnlineFirst February 2, 2015; DOI: 10.1158/1535-7163.MCT-14-0862

Table 1. Resistance profiles of 361-TM and JIMT1-TM cell lines to ADCs

ADC Treatment	Linker type	361: Parental versus TM-resistant			JIMT1: Parental versus TM-resistant		
		Parental (IC_{50}, nmol/L)	TM (IC_{50}, nmol/L)	Relative resistance	Parental (IC_{50}, nmol/L)	TM (IC_{50}, nmol/L)	Relative resistance
T_MCC_DM1 (TM-ADC)	NC	1.6	410	256×	52	820	16×
T_mc'_Aur-8261	NC	0.41	>1,000	>2,439×	10	>1,000	>100×
T_Mal'Peg_6C_2_ MMAD	NC	3.0	800	267×	52	>1,000	>19×
T_vc_MMAD	C	0.50	0.29	0.6×	13	560	43×
T_vc_Aur-8254	C	0.20	0.20	1.0×	4.8	880	183×

NOTE: Parental and TM-resistant cell lines were treated with the indicated ADCs and cytotoxicity assessed as indicated in Materials and Methods. Data are mean IC_{50} from multiple experiments ($n = 2$–26), rounded to two significant figures. Relative resistance is the ratio of the mean IC_{50} for the TM-resistant cell line versus the corresponding parental cell line.
Abbreviations: C, cleavable linker; NC, noncleavable linker.

leukemia viral oncogene homolog 2, neuro/glioblastoma derived oncogene homolog (avian).

Results

ADC resistance can be induced in cultured cancer cells

Breast cancer cell lines were selected for resistance to TM-ADC by treatment cycles at doses that were approximately the IC_{80} for the respective cell line (Supplementary Fig. S1). Parental MDA-MB-361 cells were inherently sensitive to the conjugate (IC_{50} = 1.6 nmol/L payload concentration; 0.06 μg/mL antibody concentration). However, after only approximately 1.5 months exposure cycling at 125 nmol/L TM-ADC, this population became refractory to the ADC by approximately 256-fold compared with parental cells (Table 1; Fig. 1A; and Supplementary Table S1). Interestingly, minimal cross-resistance (~3.8×) to the corresponding unconjugated drug, DM1-SMe, was observed (Table 2; Fig. 1B; structures in Supplementary Fig. S2).

The IC_{50} of TM conjugate in parental JIMT1 cells was 52 nmol/L (1.8 μg/mL antibody concentration). After approximately 3 months of selection, the IC_{50} of TM-ADC in the JIMT1-TM population increased to 820 nmol/L (27 μg/mL antibody), or approximately 16-fold higher than parental cells (Table 1; Fig. 1C; and Supplementary Table S1). The JIMT1-TM cells also showed minimal (~3.4×) loss of sensitivity to DM1-SMe (Table 2; Fig. 1D). Neither JIMT1 nor MDA-MB-361-DYT2 parental or resistant cells were inherently responsive to unconjugated trastuzumab antibody (<10% inhibition at 100 μg/mL antibody).

Significant cross-resistance was also observed to most trastuzumab ADCs composed of noncleavable linkers and delivering tubulin inhibitor payloads (representative examples in Table 1). For example, in 361-TM versus 361-parental cells, >2,000- and >200-fold reduced potency was observed to T_mc'_Aur-8261 and T_Mal'Peg_6C_2_MMAD conjugates, respectively (Table 1; Supplementary Fig. S3A and S3B), which represent auristatin/dolastatin-based payloads (Aur-8261 or MMAD) linked to trastuzumab via noncleavable linkers (24, 25 and Supplementary Fig. S2B). Reduced potency of these ADCs was also observed in the JIMT1-TM cell line compared with parental (>19× to >100× resistance; Table 1; and Supplementary Fig. S3E and S3F).

Because of the modular nature of ADCs, we hypothesized that selected modifications of the linker might restore drug sensitivity to these cells and overcome resistance. Remarkably, we observed that the 361-TM cell line retained sensitivity to payloads when

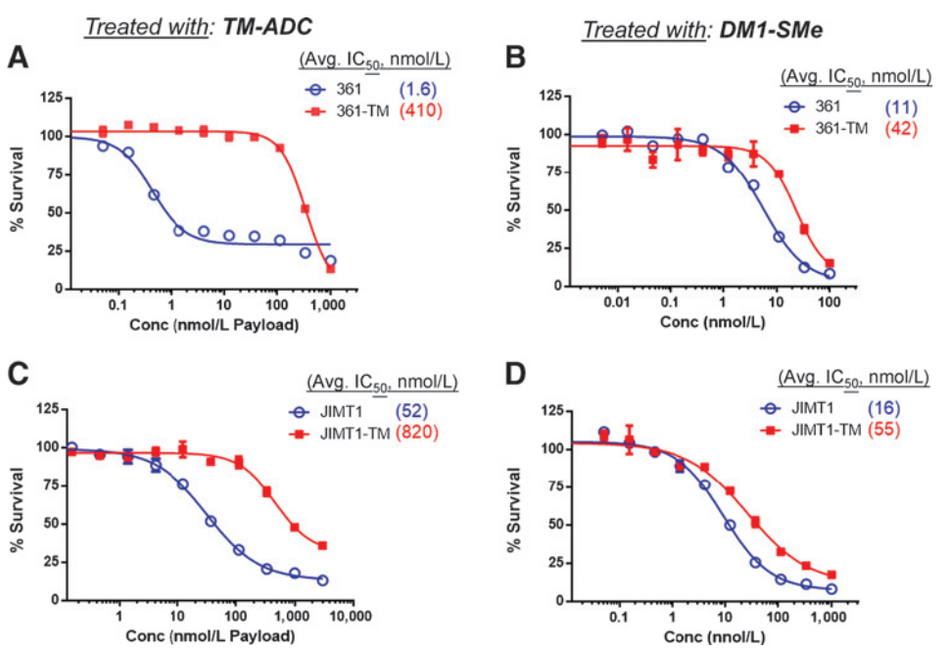

Figure 1.
Cytotoxicity profiles of parental and resistant cells treated with TM-conjugate and unconjugated drug. Cells were treated with the indicated agents for 4 days and percent survival measured by colorimetric endpoint. 361 parental (open circle) and 361-TM cells (closed square) treated with TM-ADC (A) or with unconjugated DM1-SMe (B). JIMT1 parental and JIMT1-TM cells treated with TM-ADC (C) or DM1-SMe (D). Graphs are representative of 5–26 individual experiments. Data are mean ± SD for each duplicate point (some error bars are within the size of data points). Mean IC_{50} values (nmol/L) across all experiments are indicated in the figures.

Published OnlineFirst February 2, 2015; DOI: 10.1158/1535-7163.MCT-14-0862

Table 2. Cross-resistance profile to standard-of-care chemotherapeutics and other unconjugated drugs

		361: Parental versus TM-resistant			JIMT1: Parental versus TM-resistant		
Drug class	**Treatment**	**Parental (IC_{50}, nmol/L)**	**TM (IC_{50}, nmol/L)**	**Relative resistance**	**Parental (IC_{50}, nmol/L)**	**TM (IC_{50}, nmol/L)**	**Relative resistance**
Tubulin: depolymerizing	DM1-SMe	11	42	3.8×	16	55	3.4×
	Vinblastine	2.8	2.9	1.0×	1.5	3.5	2.3×
	MMAD	0.10	0.10	1.0×	0.06	0.33	5.5×
	Aur-8254	0.44	0.42	1.0×	0.28	1.4	5.0×
Tubulin: polymerizing	Paclitaxel	5.7	7.8	1.4×	7.5	14	1.9×
	Docetaxel	3.8	5.2	1.4×	2.9	3.8	1.3×
DNA: topoisomerase inhibitors	Doxorubicin	170	410	2.4×	160	350	2.2×
	Etoposide	11,000	25,000	2.3×	4,700	13,000	2.8×
	Camptothecin	360	290	0.8×	69	160	2.3×
DNA: anti-metabolites	5-Fluorouracil	7,500	23,000	3.1×	45,000	36,000	0.8×
	Gemcitabine	25	27	1.1×	22	18	0.8×
DNA: alkylating	Oxaliplatin	13,000	4,000	0.3×	30,000	21,000	0.7×
Signaling inhibitors	Her2 kinase inhibitor	2,200	470	0.2×	1,000	1,300	1.3×
	Rapamycin analogue	5,600	3,100	0.6×	24,000	23,000	1.0×

NOTE: Parental and TM-resistant cell lines were treated with the indicated chemotherapeutic agent and cytotoxicity assessed as indicated in Materials and Methods. Data are mean IC_{50} from 2–6 determinations for each compound, rounded to 2 significant figures. Aur-8254 is an auristatin analogue. Her2 kinase inhibitor is neratinib; rapamycin analogue is temsirolimus. Relative resistance is the ratio of the mean IC_{50} for the TM-resistant cell line versus the corresponding parental cell line.

delivered via a cleavable linker, even though these drugs are functionally similar (i.e., microtubule depolymerizers). Examples of ADCs that overcome resistance are T_mcValCitPABC_MMAD and T_mcValCitPABC_Aur-8254 (Table 1; Supplementary Fig. S3C and S3D). These represent trastuzumab-based ADCs delivering either the cytotoxic payload MMAD or an auristatin analogue, Aur-8254, but where the payloads are released intracellularly by proteolytic cleavage of the mcValCitPABC ("vc") linker. While the 361-TM–resistant cell model was effectively inhibited upon treatment of such cleavable-linked ADCs, the JIMT1-TM cell line retained resistance to these ADCs (Table 1; Supplementary Fig. S3G and S3H).

To determine whether these ADC-resistant cancer cells were broadly resistant to other therapies, the 361-TM and JIMT1-TM cell models were treated with standard-of-care chemotherapeutics with various mechanisms of action. In general, small-molecule inhibitors of microtubule and DNA function remained effective against both TM-ADC–resistant cell lines (Table 2). While these cells were made resistant against an ADC delivering an analogue of the tubulin-binding compound maytansine, minimal or no cross-resistance was observed to tubulin depolymerizing or polymerizing agents. In general, the 361-TM and JIMT1-TM cells were not refractory to a broad range of cytotoxics, ruling out generic growth or cell-cycle defects that might mimic drug resistance. Hence, 361-TM cells made refractory to a TM conjugate displayed cross-resistance to microtubule inhibitor-based ADCs when delivered via noncleavable linkers, but retained sensitivity when the payload is released via cleavable proteolytic linker. In contrast, JIMT1-TM cells failed to respond broadly to trastuzumab-ADCs, suggesting a different mode of resistance between the 361-TM and JIMT1-TM cell models.

ADC resistance is maintained *in vivo*

To assess resistance *in vivo*, 361 and 361-TM cells were implanted into mice and treated with TM-ADC. In parental 361-derived tumors, 3 mg/kg of TM-ADC effectively caused regression (Fig. 2A). In contrast, 361-TM–derived tumors progressed and achieved tumors up to 1.4 g by day 69 (Fig. 2B). Tumor sizes were significantly different ($P = 0.0035$) from each other based on time-to-event analysis (Fig. 2C), supporting the observation that cells made resistant to TM-ADC *in vitro* remain refractory to the drug when grown *in vivo*. Moreover, immunohistochemistry and immunoblots confirmed detection of ABCC1 and retention of Her2 expression in the 361-TM tumors (data not shown).

Antigen expression is reduced upon chronic exposure to Her2 ADC

With respect to potential resistance mechanisms in these cell models, collectively these data suggested potential (i) loss of surface antigen and/or defects in binding, internalization, trafficking, or processing of the antibody, (ii) alterations in release of the payload from lysosomes when delivered as an ADC, (iii) differential interaction with the tubulin target, or (iv) reduced drug retention within the cell. Immunoblots of whole-cell lysates confirmed a partial decrease of Her2 in 361-TM cells, and a greater decrease of Her2 in JIMT1-TM cells (Fig. 3A, "Her2" panel). Flow cytometry showed 58% lower cell surface binding of anti-Her2 antibody in JIMT1-TM cells, and a 25% reduction in 361-TM cells (Fig. 3B). However, we did not observe any differences in the internalization rates of trastuzumab antibody (Fig. 3C) in either cell line. Because other trastuzumab-based ADCs effectively overcome resistance in 361-TM cells, reduced expression of Her2 in these cells does not likely significantly contribute to ADC resistance. In contrast, the reduced sensitivity of the JIMT1-TM cell model to most trastuzumab-based ADCs was possibly partially due to reduction of Her2 on the cell surface. To explicitly test the effect of Her2 expression on trastuzumab-ADC resistance, we transfected Her2 into JIMT1-TM cells, and this significantly resensitized the original refractory JIMT1-TM cells to multiple trastuzumab-based ADCs (Supplementary Fig. S4). These data suggest that Her2 loss is a major contributor of resistance to trastuzumab ADCs in the JIMT1-TM model.

Proteomic and transcriptional assessment identifies ABCC1 drug transporter in 361-TM cells

To determine potential mechanisms of ADC resistance by an unbiased approach, the parental and resistant cell models were characterized by cell surface proteomics and by transcriptomics. Proteins and mRNA representing multiple functional classes were altered in both cell lines and several patterns emerged. A volcano-plot depiction of surface protein changes in 361 versus 361-TM

Published OnlineFirst February 2, 2015; DOI: 10.1158/1535-7163.MCT-14-0862

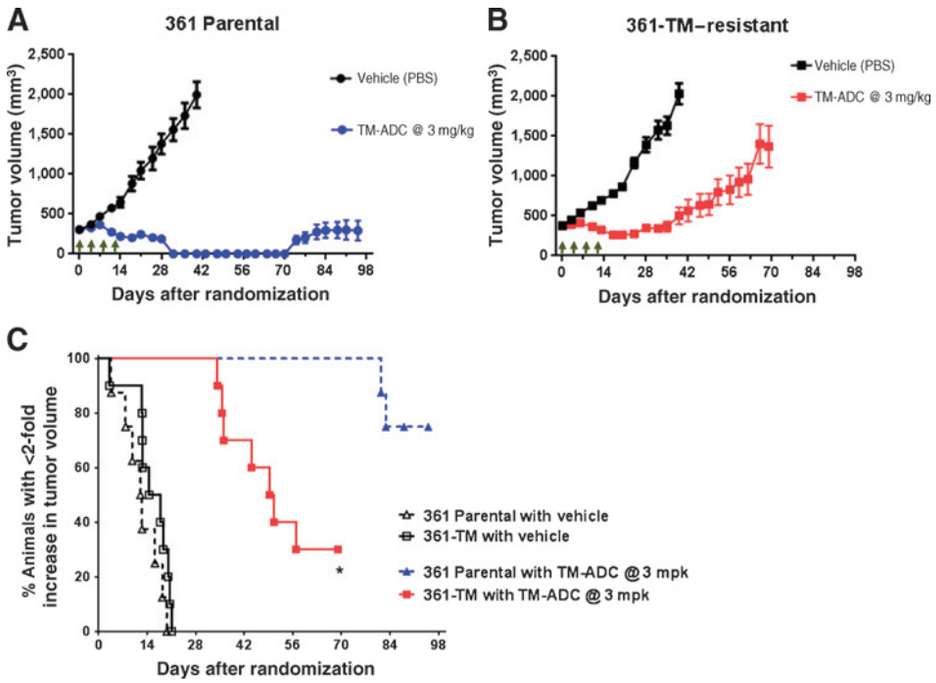

Figure 2.
Tumors derived from 361-TM cells are refractory to TM-ADC *in vivo* compared with parental 361 tumors. Cells from 361 (A) and 361-TM (B) models were implanted into NSG mice and treated with 3 mg/kg of TM-ADC on days 0, 4, 8, and 12 (arrows). Data are mean ± SEM of tumor size on each measurement day. C, time-to-event Kaplan–Meier plot for 2-fold increases from baseline of tumor size. *, $P < 0.005$ between 361-TM compared with 361 ADC treated groups, by log-rank test.

cells is represented in Supplementary Fig. S5. One protein with high abundance in the 361-TM–resistant cells relative to parental 361 cells was the drug transporter ABCC1 (MRP1) (Fig. 4A, right). Transcriptional profiling supported the observation of increased RNA levels of ABCC1 (Fig. 4B, right). Immunoblots verified ABCC1 overexpression in 361-TM relative to 361-parental cells (Fig. 3A, "ABCC1"). Flow cytometry confirmed increased binding with anti-ABCC1 antibody (Fig. 3D), and a general increase of drug efflux in 361-TM cells (Fig. 3E). To determine whether ABCC1 might contribute to TM-ADC resistance, we used the drug transporter reversal agent reversan, which is reported to be relatively selective for ABCC1 (MRP1) and ABCB1 (MDR1) efflux compared with other transporters (26). Remarkably, increasing concentrations of reversan sensitized 361-TM cells to TM-ADC back to the level of parental cells (Fig. 5A). As a control, reversan was tested in parental cells and a partial shift in sensitivity of 4-fold was observed (Fig. 5B). In addition, siRNA-mediated knockdown of ABCC1 in 361-TM cells increased the response to trastuzumab ADCs (Supplementary Fig. S6), further supporting a role for this drug pump in ADC resistance.

To address whether TM-ADC or free DM1 showed reduced activity in another ABCC1-expressing cell line, we obtained the H69 and H69AR isogenic cell pair. We confirmed previously reported ABCC1 expression in H69AR cells (ref. 27; Fig. 3A, "ABCC1") and detected levels higher than in 361-TM cells. Cytotoxicity studies in H69AR confirmed 22-fold resistance to doxorubicin, a benchmark ABCC1 substrate. Unconjugated DM1 also showed 40-fold reduced potency in H69AR, suggesting that DM1 is effluxed in high ABCC1-expressing cells (Supplementary Table S2).

Cumulatively, these data suggest that ABCC1 can mediate resistance to DM1 and TM-ADC; however, alone, they do not explain the approximately 250-fold resistance observed to TM-ADC, the high level of cross-resistance to other ADCs with auristatin payloads that are not ABCC1 substrates, and the minimal resistance to free DM1 (3.8×) and doxorubicin (2.4×) in 361-TM cells. One possible explanation is that the modified released products of noncleavable ADCs may be slightly better substrates of ABCC1 than the noncapped payloads. Results with the H69 and H69AR pair (Supplementary Table S2) suggest slightly higher resistance ratios for Cys-capped metabolites (i.e., Cys_mc_MMAD, etc.) compared with the unmodified auristatins (i.e., MMAD); however, interpretation is difficult due to impermeability of these metabolites and their high IC_{50}. Notably, we observed that long-term ADC treatment of 361-TM cells resulted in broad proteomic and transcriptional changes. For example, gene set enrichment analysis of proteomic profiling data from 361-TM cells indicates upregulation of proteins from several diverse pathways, including membrane trafficking, endocytosis, integrin signaling, and metabolism (data not shown), suggesting that although drug efflux is likely the dominant mechanism of ADC resistance in this model, other pathways have been altered as a result of chronic TM-ADC treatment.

Trafficking and signaling proteins are altered in JIMT1-TM ADC-resistant cells

In JIMT1-TM cells, a different spectrum of protein and mRNA changes was observed upon profiling. Decreased Her2 was evident at the protein and RNA levels (Fig. 4C and 4D, respectively), implicating a transcriptional mechanism of downregulation possibly due to chronic exposure to antibody. No differences in ABC drug transporter expression were detected in this cell population. Pairwise comparison of proteins in the endosome and lysosome gene sets revealed a trend where JIMT1-TM cells displayed a disproportionately higher number of such proteins with elevated abundance compared with JIMT1 (Supplementary Fig. S7A and S7B). These proteins include Ras-related protein Rab5B, autophagy-related protein 9A (ATG9A), and huntingtin (HTT), which are involved in lysosome/endosome biogenesis and/or vesicle transport. In addition, RAB GTPase activating protein 1

Published OnlineFirst February 2, 2015; DOI: 10.1158/1535-7163.MCT-14-0862

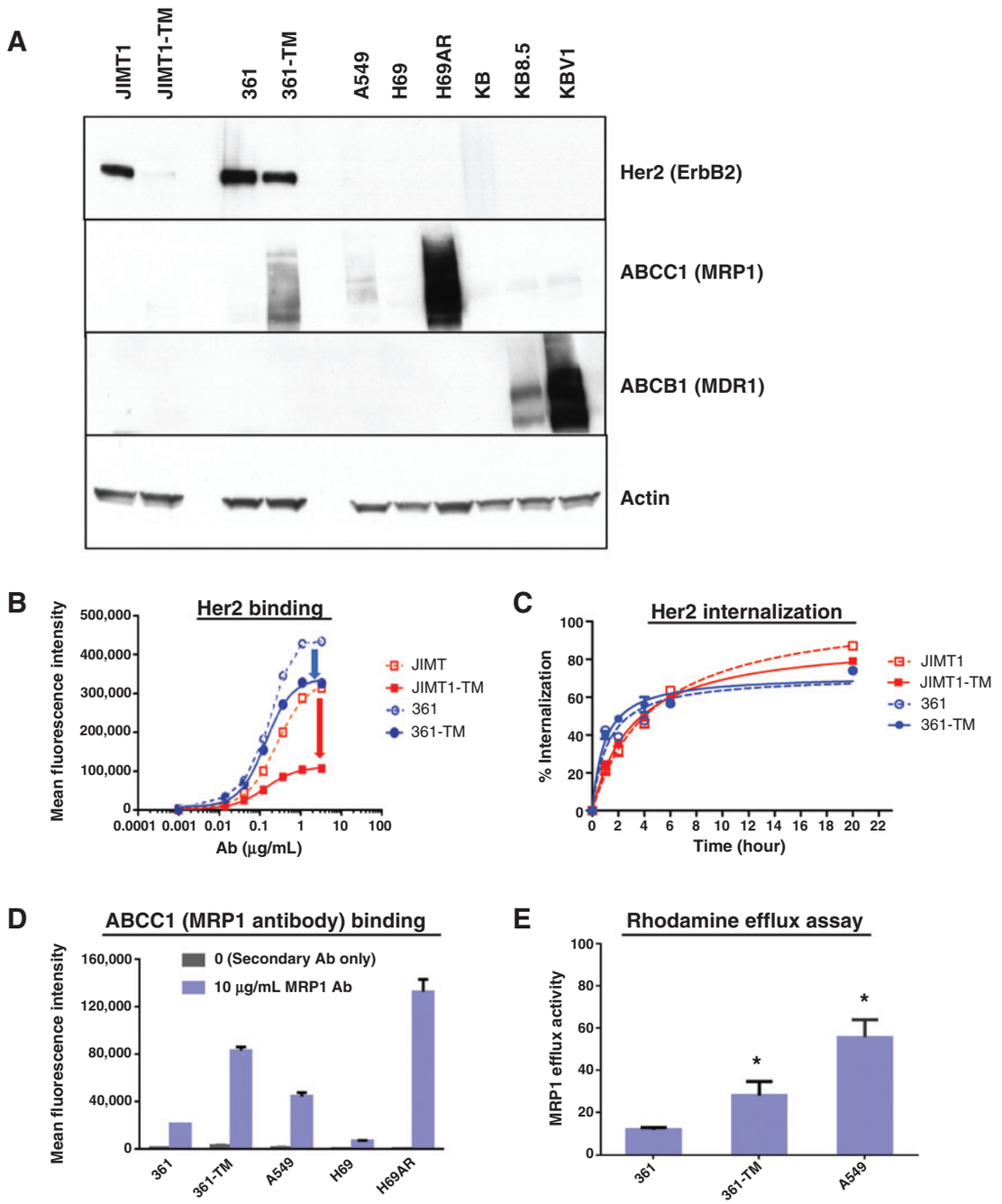

Figure 3.
Expression of Her2 and drug efflux proteins in parental and resistant cell models. A, immunoblot analyses of 80 μg total protein from whole-cell lysates show Her2 levels decreased in JIMT1-TM cells and partially reduced in 361-TM cells. ABCC1 (MRP1) expression is elevated in 361-TM cells, but not in JIMT1-TM cells or in their parental counterparts. A549 and H69AR cells serve as positive controls for ABCC1. No detectable ABCB1 (MDR1) was observed in either 361-TM or JIMT1-TM cells, compared with positive controls KB-8.5 and KB-V1 cells. Cell lines were analyzed by flow cytometry for trastuzumab antibody binding (B) and internalization (C). 361, blue lines; JIMT1, red lines; parental cells, open symbols; TM-ADC–resistant cells, closed symbols. D, flow cytometric analysis of ABCC1 antibody shows elevated binding in 361-TM cells relative to parental 361 cells. Secondary antibody only (gray bar); 10 μg/mL ABCC1 antibody (blue bar). E, efflux study demonstrates increased accumulation of rhodamine in 361-TM cells compared with parental cells in the presence of reversan. *, $P < 0.001$ difference compared with 361 cells as evaluated by Student *t* test. Reference cell lines A549 and H69AR express ABCC1.

(RABGAP1/Rab6), implicated in microtubule-mediated transport of vesicles (28), and serine/threonine-protein kinase PAK4, which supports GTPase activity associated with cytoskeleton reorganization (29), were among the highest expressed proteins in JIMT1-TM cells upon plasma membrane proteomic profiling, and their increased surface association was confirmed by

Published OnlineFirst February 2, 2015; DOI: 10.1158/1535-7163.MCT-14-0862

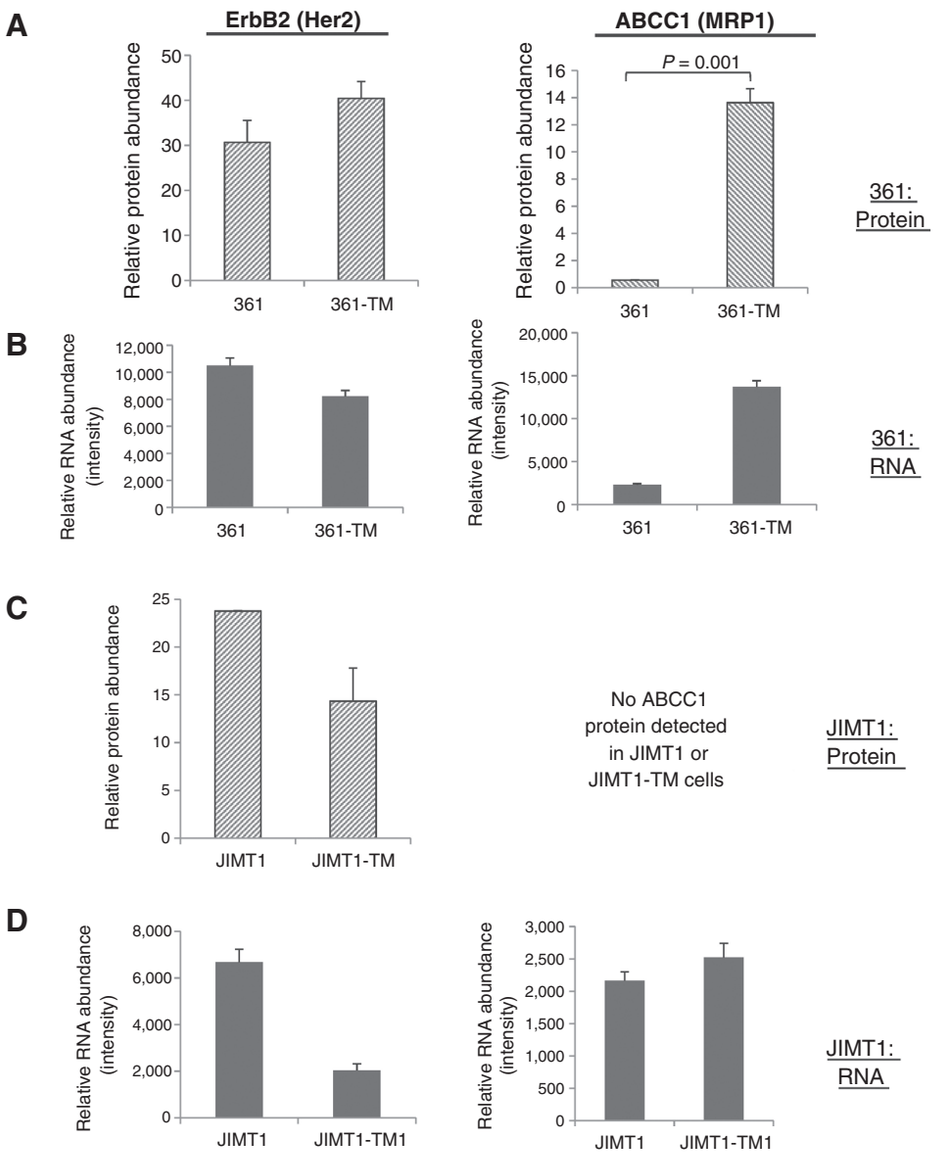

Figure 4.
Levels of Her2 and ABCC1 observed by cell surface proteomic profiling and transcriptional profiling of parental and ADC-resistant cell lines. A, protein expression from cell surface proteomic profiling of 361 versus 361-TM cells for Her2 and ABCC1. B, RNA expression from transcriptional profiling of 361 versus 361-TM cells of *erbb2* and *ABCC1*. C, cell surface protein expression of Her2 from surface proteomic profiling of JIMT1 versus JIMT1-TM. No ABCC1 was detected by surface proteomics in JIMT1 or JIMT1-TM cells. D, RNA expression from transcriptional profiling of JIMT1 versus JIMT1-TM of *erbb2* and *ABCC1*. Protein levels from cell surface proteomic profiling (A and C) are expressed as average relative protein abundance spectral counts; error bars represent SD between replicate samples. RNA expression from transcriptional profiling by microarray (B and D); error bars represent SD between triplicate samples. Data are for ErbB2 (Her2; left) and ABCC1 (MRP1; right).

immunoblot (Supplementary Fig. S8). Taken together, these data suggest potential general alterations in regulation of actin/microtubule cytoskeleton and endosome/lysosome pathways in JIMT1-TM cells that may have been perturbed upon chronic TM-ADC exposure.

ADC trafficking and metabolites are altered in resistant cells

To further evaluate the hypothesis that altered trafficking and/or endolysosomal activities might contribute to TM-ADC resistance in the 361-TM and JIMT1-TM models, ADC trafficking was evaluated by live cell imaging microscopy. Two different ADCs were used for these studies; both conjugates contained an auristatin with a covalently attached BODIPY fluorescent probe; however, the ADCs differed by linker type: noncleavable linker (T_mc_Aur-BODIPY) versus cleavable linker (T_mcValCitPABC_Aur-BODIPY). In both 361 and JIMT1 parental cells, noncleavable-linked ADC colocalized with lysosome over time, which is expected upon lysosomal processing (Supplementary Fig. S9A and S9D, closed squares). In contrast, the cleavable-linked ADC showed minimal colocalization with lysosome (Supplementary Fig. S9A and S9D, open squares), consistent with cleavage of mcValCitPABC linker and processing of the fluorescently labeled payload in a compartment before reaching the lysosome (A. Xavier and C. May, publication pending).

We next assessed trafficking patterns using the TM-ADC–resistant cell lines. In the presence of an ADC containing a cleavable-linked fluorescent probe, 361-TM cells showed identical low colocalization of ADC with lysosomes as observed with parental 361 cells (Supplementary Fig. S9B). This result parallels the observed sensitivity of 361-TM cells to cleavable-linked ADCs and suggests that cleavable-linked ADCs are processed correctly in 361-TM cells. Interestingly, 361-TM cells showed increased colocalization of the noncleavable linked ADC probe with lysosome at later time points, as compared with parental 361 cells

Published OnlineFirst February 2, 2015; DOI: 10.1158/1535-7163.MCT-14-0862

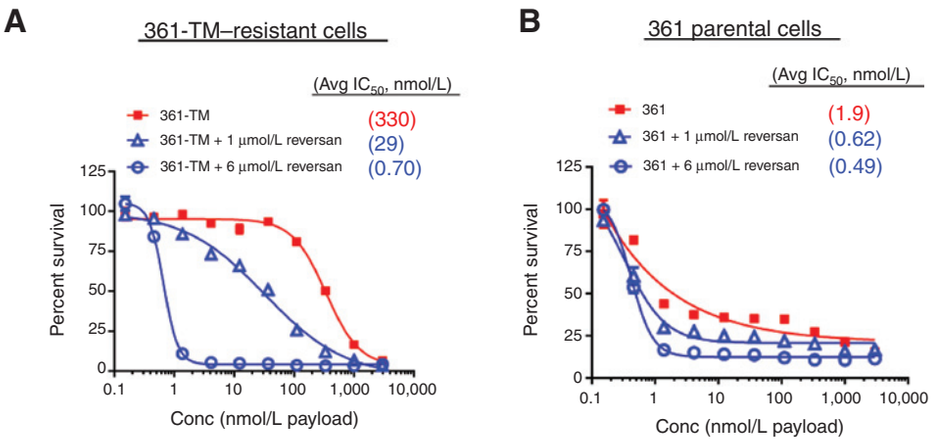

Figure 5.
Reversal of resistance to TM-conjugate by pharmacologic block of ABCC1 transporter. Effect of absence (red square) or presence of ABCC1 reversal agent, reversan, at 1 μmol/L (blue triangle) and 6 μmol/L (blue circle) on 361-TM cells (A) and 361-parental cells (B) in the presence of a serial dilution of TM-ADC.

(Supplementary Fig. S9C). These data were determined to be statistically significant at several time points, as indicated in the figure, although not for extended times. Hence, this suggests a possible contribution of defective processing of noncleavable linked ADCs, with increased retention in the lysosome over time.

For JIMT1-TM cells, both the cleavable (Supplementary Fig. S9E) and noncleavable (Supplementary Fig. S9F) linked ADCs colocalized with lysosomes at late time points. These data suggest potential contribution of incomplete processing of the ADC, with failure to degrade or release the fluorescently labeled payload from the lysosomal compartment, as compared with parental cells. Representative images of these trafficking data at 0 and 6 hours are provided in Supplementary Fig. S9G. In addition to the labeled ADC approach to study trafficking, receptor recycling studies were conducted as previously reported (30). Enhanced recycling of TM-ADC–bound Her2 complex was observed in JIMT1-TM cells compared with JIMT1 parental cells, yet recycling of the unrelated transferrin receptor was not affected (Supplementary Fig. S10A and S10B).

As a result of the observed alterations of ADC trafficking, we monitored the respective putative released payload products of representative noncleavable and cleavable linked ADCs in these cells. We observed the expected linker–payload metabolites in cellular extracts of all four cell lines, and all metabolites were decreased in the resistant compared with the respective parental cells (Supplementary Fig. S11A and S11B). The magnitude of the changes was similar to the decreased levels of Her2 protein in 361-TM and JIMT1-TM cells; hence, it is not clear whether the decrease is due to reduced antigen levels or reduced ADC processing. Supplementary Table S3 summarizes the observed differences in resistance profile, Her2 levels, trafficking, and released species in 361-TM and JIMT1-TM cells compared with respective parental cell lines.

Discussion

Breast cancer cell lines were made resistant to TM conjugate by chronic cycling at high doses over several months. Differences in resistance profiles were observed, suggesting unique mechanisms of resistance that likely depend upon the cancer cell genetic background. The 361-TM and JIMT1-TM cell models were more fully characterized and both retained sensitivity to unconjugated maytansine analogue but were refractory to TM-ADC. Moreover, neither cell line was markedly resistant to most standard-of-care chemotherapeutics, including other tubulin inhibitors. Remarkably, despite high cross-resistance to many ADCs, 361-TM cells responded to conjugates delivering payload via cleavable linkers. Unbiased approaches of cell surface proteomics and transcriptional profiling identified changes in protein and RNA signatures associated with multiple pathways in these refractory cell lines, with reduction of Her2 in JIMT1-TM and induction of drug transporter ABCC1 in 361-TM as likely primary mediators of ADC resistance in each respective cell model.

For the JIMT1-TM cells, decreased Her2 antigen likely contributes to the poor cytotoxic response to trastuzumab ADCs. The parental JIMT1 cell line was originally derived from a patient failing trastuzumab antibody therapy; *erbB2* was reportedly amplified yet Her2 protein levels are only moderate in the cell line (20). Further characterization demonstrated that JIMT1 express mucin MUC4, partially masking the trastuzumab epitope (31), and have an activating PI3KCA mutation and low PTEN (32). Despite abrogated response to trasuzumab antibody, JIMT1 cells retain responsiveness to DM1-conjugated trastuzumab ADCs both *in vitro* (this report) and *in vivo* (33). In the current clinical setting, many patients receive trastuzumab before trastuzumab-DM1 ADC; hence, the JIMT1 cell model was used to determine whether there may be differences in resistance mechanisms to ADC following failure of first-line antibody therapy. Indeed, upon chronic cycling exposure of JIMT1 cells to a trastuzumab ADC, resistance to the ADC developed. Downregulation of Her2 likely contributes to a majority of the resistance phenotype to trastuzumab-based ADCs in the JIMT1-TM model, although proteomics also identified other surface protein and lysosomal alterations. Her2 receptor levels are reported to be maintained or decreased in patient tumors during treatment with trastuzumab antibody (34, 35); however, no data are yet reported upon chronic T-DM1 ADC therapy. Importantly, other unconjugated chemotherapeutics retained activity in JIMT1-TM in the current study, even those operating by tubulin inhibition, allowing the option of alternative therapy following tumor progression.

For the 361-TM–resistant model, the partial decrease in Her2 likely does not significantly mediate resistance because other trastuzumab-based ADCs overcome resistance. Induction of drug transporter ABCC1 (MRP1) was evident at protein and RNA levels, and inhibition of ABCC1 by pharmacologic and RNA interference methods rescued the response to TM-ADC. ABCB1

Published OnlineFirst February 2, 2015; DOI: 10.1158/1535-7163.MCT-14-0862

(MDR1), which can efflux various tubulin inhibitors and other drugs, was not observed in these cells. Nevertheless, 361-TM cells retained sensitivity to doxorubicin and free DM1, which we confirmed are ABCC1 substrates. This suggests that the level of ABCC1 in 361-TM cells may be too low to mediate resistance to unconjugated DM1, but that the ADC-processed form of the drug may be a superior substrate compared with free drug. Payload release from ADCs with noncleavable linkers, such as MCC or maleimidocaproyl, is expected to occur only following antibody degradation within the proteolytic lysosome, resulting in Lys- or Cys-capped linker–payload (i.e., Lys_MCC_DM1 or Cys_mc_Aur; refs. 36, 37). These modified metabolites have reduced membrane permeability and possibly enhanced association with drug transporter proteins. Several Cys-capped linker payloads were less effective in H69AR cells, a very high ABCC1-expressing line. Unexpectedly, 361-TM cells retained sensitivity to trastuzumab conjugates containing a cleavable linker, suggesting that the released cytotoxic payload product (which is not amino acid capped) is able to evade resistance. Moreover, other nontubulin payloads delivered by trastuzumab (data not shown) are also effective. This has important implications for the treatment of ADC-resistant tumors with antibodies delivering alternative linkers and/or payloads, and the need to understand how their metabolites are processed.

The emergence of drug resistance is a complex process. Chronic drug pressure on cancer cells likely forces the cell to attempt many simultaneous escape routes to evade the cytotoxic effects of the therapeutic. Once an effective mechanism develops and the cell adapts, it is possible that other markers may remain as evidence of those selection attempts. We hypothesize that in these cell lines, the mechanisms of resistance to TM-ADC observed were "low threshold" mechanisms during chronic exposure to this drug. Parental 361 cells express very low but detectable levels of ABCC1 RNA and protein; hence, this efflux protein was able to be further induced upon chronic drug exposure. In JIMT1 cells originally isolated from trastuzumab-treated patients, only moderate levels of Her2 are observed despite gene amplification, hence chronic exposure to trastuzumab-ADC appears to have contributed to further reduced receptor levels. The distinct mechanisms of T-DM1 resistance observed by Phillips and colleagues (17) in two other breast cancer cell lines (and different from the mechanisms identified in our two breast cancer cell lines) suggests that each cancer cell will adapt to a given drug based on its biology. We also propose that the measurable changes in proteins associated with various cellular pathways identified by proteomics in both 361-TM and JIMT1-TM cells may be evidence of other attempts at resistance upon chronic exposure of these cells to an ADC containing a tubulin inhibitor.

Unlike free drugs that enter cells by passive diffusion, ADCs require antigen-dependent binding and intact endolysosomal trafficking for the payload to access its intracellular target. Ineffectiveness of an immunoconjugate may be due to defective ADC trafficking within the endosome/lysosome, incomplete degradation of antibodies, and/or impaired export of drug from these organelles. In addition, TM-ADC delivers a microtubule depolymerizing agent, and chronic treatment with this drug may alter tubulin dynamics and pathways associated with trafficking. In both 361-TM and JIMT1-TM models, gene set enrichment indicated alterations of proteins involved in membrane trafficking, vesicle transport, and endoplasmic reticulum to golgi transport, in addition to other pathways. For example, in 361-TM cells, we observed several upregulated proteins (e.g., SEC31A, CHMP4B, SEC24, VTA1) and these are reported to be associated with vesicle budding and endosomal sorting (38). In JIMT1-TM cells, Rab5B, Rab21, and other Rab members were either up- or downregulated; these proteins control endosome dynamics by recruiting microtubule motors to endosomes (39). Many proteins associated with vesicular GTPase activity and actin dynamics were overrepresented in JIMT1-TM cells, including RABGAP1, kinases ROCK1 and ROCK2, profilin PFN1, and actin-related proteins ARPC1A and ARPC3. These protein and RNA changes were observed upon broad profiling of these cell models, and it is not clear whether any of these affect the drug resistance phenotype. However, it is provocative to speculate that a cancer cell may attempt to overcome persistent treatment with an ADC by interfering with processes that mediate internalization and processing of the drug. In addition to changes in the trafficking proteome of the resistant cell lines, live image microscopy detected enhanced localization of fluorescently labeled noncleavable linked-ADCs with the lysosome in 361-TM and JIMT1-TM cells compared with parental cells. Metabolomic assessment of the resistant cell lines also showed reduced amounts of released species from the treatment ADCs, possibly due to reduced antigen, drug efflux, or ADC-processing defects.

In addition to changes in trafficking proteins, proteomic profiling of 361-TM and JIMT1-TM cells showed alterations in proteins involved in posttranslational modification, including ubiquitinating enzymes (e.g., HECTD1, USP4, STUB1), kinases (e.g., Src, ATM), and phosphatases (e.g., PTPN23, PTPN11). For example, ubiquitin ligase HECTD1 was increased more than 8-fold in JIMT1-TM compared with parental JIMT1, and its association with the cell surface was verified by immunoblot (Supplementary Fig. S8). HECTD1 is a member of the E3 ubiquitin ligase family of enzymes that regulate ubiquitin specificity (40) and cellular migration (41). In general, ubiquitylation is critical for endocytosis, sorting, and trafficking of membrane proteins, and HECT family and other ubiquitin ligases are involved in this process (39, 40). Hence, altered regulation of vesicle or receptor trafficking by ubiquitylation may be used by cancer cells attempting to evade chronic ADC treatment. The impact of targeted downregulation of these RNA and proteins on ADC resistance is currently under investigation.

In studying resistance to the trastuzumab-ADC, we also considered potential contributions of resistance mechanisms that have been observed to trastuzumab (Herceptin) antibody in the clinic and in cultured cell systems. One reported mechanism of resistance to Herceptin antibody is the compensated overexpression of EGFR, IGF1R, or ErbB ligands (42–44). In some cases, increased sensitivity to other ErbB-family kinase inhibitors was observed (45). In our studies, surface profiling proteomics did not detect elevation of these proteins in 361-TM or JIMT1-TM models. Interestingly, in 361-TM cells we observed 5-fold increased sensitivity to Her2-specific kinase inhibitor, neratinib (Table 2), as well as increased sensitivity to other pan-ErbB-family kinase inhibitors. This effect may be related to changes in receptor signaling in 361-TM cells, but this sensitivity was not observed in JIMT1-TM. In patients with breast cancer, ErbB kinase inhibitors were effective after progression on trastuzumab (46) and suggests an additional therapeutic approach to inhibit trastuzumab-ADC refractory cancer. Downregulation of PTEN or increased PI3K signaling is reported in cultured cell

Published OnlineFirst February 2, 2015; DOI: 10.1158/1535-7163.MCT-14-0862

systems and in some patient tumors refractory to Herceptin antibody, and PI3K inhibitors can rescue trastuzumab resistance *in vitro* and *in vivo* (47, 48). We observed no differential (<2-fold) in sensitivity to PI3K small-molecule inhibitors, and proteomic and transcriptional profiling did not identify altered PI3K or PTEN protein or RNA. Both cell lines used for this study reportedly possess PIK3CA mutations; the PIK3CA-E545K mutation, reported in MDA-MB-361 cells, is suggested to contribute to resistance to Herceptin antibody (47), but clearly does not predispose parental 361 cells to inherent resistance to trastuzumab-ADC.

We have developed cancer cell lines with acquired resistance to a TM ADC. Resistance to TM-ADC translated *in vivo* in the 361-TM model. Proteomic and transcriptional profiling enabled an unbiased assessment of molecular changes in these refractory cell models. Induction of drug transporter ABCC1 or reduction of Her2 antigen are two mechanisms that appear to affect the responsiveness of two different cell lines to TM-ADC. In addition, alterations in proteins involved in vesicle transport, cytoskeletal function, phosphosignaling, ubiquitylation, and other pathways were observed, and suggest ways by which cells respond to chronic ADC/tubulin inhibitor-based therapy. The types of responses observed in 361-TM and JIMT1-TM cells are consistent with emerging data in our lab on additional cellular models of ADC resistance, and such diversity of response would be expected in heterogeneous cancer cell populations. Interestingly, the types of responses that are emerging among cultured cell models of ADC resistance are converging on antigen downregulation, drug efflux pumps, and altered signaling/trafficking pathways. We refer to data from three independent labs (refs. 17, 19; and our lab) where collectively at least 10 different cell models have demonstrated at least one of these three pathways altered for the clinically approved ADCs Kadcyla or Adcetris. It is not known whether these mechanisms will also be detected in the tumors of patients failing ADC therapy; one challenge is that pre- and posttreatment patient biopsy samples of solid tumors are difficult to obtain and variation in responses will likely require large sample numbers to statistically power any conclusions. However, these new ADC-refractory cell models can serve as tools to interrogate molecular mechanisms that may contribute to resistance to immunoconjugate therapy and provide potential biomarkers to evaluate in patient tumors once large numbers of tumor samples are accessible.

ADCs are emerging as effective biotherapeutics for the treatment of cancer. The modular nature of ADCs allows the delivery of linker–payload combinations via different antibodies to cancer cells. Importantly, we have observed that changes to the linker can overcome acquired resistance to a TM-ADC and achieve cytotoxicity of the same cancer cell population. This effect will likely depend upon the cancer cell genetic background, as two different cultured cancer cell models of TM-ADC resistance showed varied responses with this "component switching" approach. It is possible that patients whose tumors become refractory to one therapy may respond to another ADC, even directed against the same target antigen. Hence, an antigen-based biomarker patient selection strategy may remain intact if ADCs with various modes of linker release and/or varied payload analogues are approved for clinical use.

Disclosure of Potential Conflicts of Interest

No potential conflicts of interest were disclosed.

Authors' Contributions

Conception and design: F. Loganzo
Development of methodology: F. Loganzo, X. Tan, J.S. Myers, E. Graziani
Acquisition of data (provided animals, acquired and managed patients, provided facilities, etc.): F. Loganzo, X. Tan, M. Sung, G. Jin, J.S. Myers, F. Wang, V. Diesl, S. Musto, M.-H. Lam, K. Khandke, K.S.K. Kim, M. Cinque, E. Graziani
Analysis and interpretation of data (e.g., statistical analysis, biostatistics, computational analysis): F. Loganzo, X. Tan, M. Sung, J.S. Myers, E. Melamud, M.T. Follettie, J. Lucas, E. Graziani, C.J. O'Donnell, K.T. Arndt
Writing, review, and/or revision of the manuscript: F. Loganzo, M. Sung, J.S. Myers, C.J. O'Donnell, K.T. Arndt
Administrative, technical, or material support (i.e., reporting or organizing data, constructing databases): F. Loganzo, J.S. Myers, W. Hu, A. Maderna
Study supervision: F. Loganzo, J. Lucas, H.-P. Gerber
Other (reagent preparation): M.B. Charati

Acknowledgments

The authors appreciate the contributions of Pfizer colleagues Ellie Muszynska, Nadira Prashad, Anton Xavier, Chad May, Jon Golas, Fan Jiang, Emily Emmet, and Anna Maria Barbuti for excellent technical assistance, Fred Immerman for statistical analyses, and Puja Sapra and Dangshe Ma for critical review of the article. The authors also thank Christine Hosselet for facilitating authentication of the cell lines, Ed Rosfjord for time-to-event analysis of the *in vivo* results, Pfizer Worldwide Medicinal Chemistry colleagues Russell Dushin, Chakrapani Subramanyam, Frank Koehn, Sai Chetan Sukuru, and their teams for helpful discussions and for the design and synthesis of all of the linker–payloads, the released species, the BODIPY-labeled auristatin ADCs, and several conjugates prepared to enable these studies.

The costs of publication of this article were defrayed in part by the payment of page charges. This article must therefore be hereby marked *advertisement* in accordance with 18 U.S.C. Section 1734 solely to indicate this fact.

Received October 3, 2014; revised January 19, 2015; accepted January 22, 2015; published OnlineFirst February 2, 2015.

References

1. Lambert JM, Chari RV. Ado-trastuzumab Emtansine (T-DM1): an antibody-drug conjugate (ADC) for HER2-positive breast cancer. J Med Chem 2014;57:6949–64.
2. Francisco JA, Cerveny CG, Meyer DL, Mixan BJ, Klussman K, Chace DF, et al. cAC10-vcMMAE, an anti-CD30-monomethyl auristatin E conjugate with potent and selective antitumor activity. Blood 2003;102:1458–65.
3. Sapra P, Hooper AT, O'Donnell CJ, Gerber HP. Investigational antibody drug conjugates for solid tumors. Expert Opin Invest Drugs 2011;20:1131–49.
4. Holohan C, Van Schaeybroeck S, Longley DB, Johnston PG. Cancer drug resistance: an evolving paradigm. Nature Rev Cancer 2013;13:714–26.
5. de Jonge-Peeters SD, Kuipers F, de Vries EG, Vellenga E. ABC transporter expression in hematopoietic stem cells and the role in AML drug resistance. Crit Rev Oncol Hematol 2007;62:214–26.
6. Fletcher JI, Haber M, Henderson MJ, Norris MD. ABC transporters in cancer: more than just drug efflux pumps. Nature Rev Cancer 2010;10:147–56.
7. Szakacs G, Paterson JK, Ludwig JA, Booth-Genthe C, Gottesman MM. Targeting multidrug resistance in cancer. Nat Rev Drug Discov 2006;5:219–34.
8. Kavallaris M. Microtubules and resistance to tubulin-binding agents. Nature Rev Cancer 2010;10:194–204.
9. Loganzo F, Hari M, Annable T, Tan X, Morilla DB, Musto S, et al. Cells resistant to HTI-286 do not overexpress P-glycoprotein but have reduced

drug accumulation and a point mutation in alpha-tubulin. Mol Cancer Ther 2004;3:1319–27.
10. Engelman JA, Settleman J. Acquired resistance to tyrosine kinase inhibitors during cancer therapy. Curr Opin Genet Dev 2008;18:73–9.
11. Zhang J, Yang PL, Gray NS. Targeting cancer with small molecule kinase inhibitors. Nature Rev Cancer 2009;9:28–39.
12. Nahta R, Esteva FJ. Herceptin: mechanisms of action and resistance. Cancer Lett 2006;232:123–38.
13. Dokmanovic M, Hirsch DS, Shen Y, Wu WJ. Rac1 contributes to trastuzumab resistance of breast cancer cells: Rac1 as a potential therapeutic target for the treatment of trastuzumab-resistant breast cancer. Mol Cancer Ther 2009;8:1557–69.
14. Bergers G, Hanahan D. Modes of resistance to anti-angiogenic therapy. Nature Rev Cancer 2008;8:592–603.
15. Starling JJ, Maciak RS, Hinson NA, Hoskins J, Laguzza BC, Gadski RA, et al. *In vivo* selection of human tumor cells resistant to monoclonal antibody-Vinca alkaloid immunoconjugates. Cancer Res 1990;50:7634–40.
16. Barok M, Joensuu H, Isola J. Trastuzumab emtansine: mechanisms of action and drug resistance. Breast Cancer Res 2014;16:R22.
17. Phillips GL. Mechanisms of acquired resistance to Trastuzumab emtansine (T-DM1). World ADC Summit; 2011 Oct 25- 28; San Francisco, CA: London: Hanson Wade Limited.
18. Phillips GD, Fields CT, Li G, Dowbenko D, Schaefer G, Miller K, et al. Dual targeting of HER2-positive cancer with trastuzumab emtansine and pertuzumab: critical role for neuregulin blockade in antitumor response to combination therapy. Clin Cancer Res 2014;20:456–68.
19. Lewis TS, Gordon K, Li F, Weimann A, Bruders R, Miyamoto JB, et al. Characterization and circumvention of drug resistance mechanisms in SGN-35-resistant HL and ALCL clonal cell lines [abstract]. In: Proceedings of the 105th Annual Meeting of the American Association for Cancer Research; 2014 Apr 5–9; San Diego, CA: Philadelphia (PA): AACR.
20. Tanner M, Kapanen AI, Junttila T, Raheem O, Grenman S, Elo J, et al. Characterization of a novel cell line established from a patient with Herceptin-resistant breast cancer. Mol Cancer Ther 2004;3:1585–92.
21. Chari RV, Martell BA, Gross JL, Cook SB, Shah SA, Blattler WA, et al. Immunoconjugates containing novel maytansinoids: promising anticancer drugs. Cancer Res 1992;52:127–31.
22. Schwender H. siggenes: Multiple testing using SAM and Efron's empirical Bayes approaches. R package version 1.32.0 ed2012.
23. Wang J, Duncan D, Shi Z, Zhang B. WEB-based GEne SeT AnaLysis Toolkit (WebGestalt): update 2013. Nucleic Acids Res 2013;41:W77–83.
24. Maderna A, Doroski M, Subramanyam C, Porte A, Leverett CA, Vetelino BC, et al. Discovery of Cytotoxic Dolastatin 10 Analogues with N-Terminal Modifications. J Med Chem 2014;57:10527–43.
25. Tumey LN, Charati M, He T, Sousa E, Ma D, Han X, et al. Mild method for succinimide hydrolysis on ADCs: impact on ADC potency, stability, exposure, and efficacy. Bioconjug Chem 2014;25:1871–80.
26. Burkhart CA, Watt F, Murray J, Pajic M, Prokvolit A, Xue C, et al. Small-molecule multidrug resistance-associated protein 1 inhibitor reversan increases the therapeutic index of chemotherapy in mouse models of neuroblastoma. Cancer Res 2009;69:6573–80.
27. Mirski SE, Gerlach JH, Cole SP. Multidrug resistance in a human small cell lung cancer cell line selected in adriamycin. Cancer Res 1987;47:2594–8.
28. Grigoriev I, Splinter D, Keijzer N, Wulf PS, Demmers J, Ohtsuka T, et al. Rab6 regulates transport and targeting of exocytotic carriers. Developmental Cell 2007;13:305–14.
29. Callow MG, Zozulya S, Gishizky ML, Jallal B, Smeal T. PAK4 mediates morphological changes through the regulation of GEF-H1. J Cell Sci 2005;118:1861–72.
30. Scott DB, Michailidis I, Mu Y, Logothetis D, Ehlers MD. Endocytosis and degradative sorting of NMDA receptors by conserved membrane-proximal signals. J Neurosci 2004;24:7096–109.
31. Nagy P, Friedlander E, Tanner M, Kapanen AI, Carraway KL, Isola J, et al. Decreased accessibility and lack of activation of ErbB2 in JIMT-1, a herceptin-resistant, MUC4-expressing breast cancer cell line. Cancer Res 2005;65:473–82.
32. Koninki K, Barok M, Tanner M, Staff S, Pitkanen J, Hemmila P, et al. Multiple molecular mechanisms underlying trastuzumab and lapatinib resistance in JIMT-1 breast cancer cells. Cancer Lett 2010;294:211–9.
33. Barok M, Tanner M, Koninki K, Isola J. Trastuzumab-DM1 causes tumour growth inhibition by mitotic catastrophe in trastuzumab-resistant breast cancer cells *in vivo*. Breast Cancer Res 2011;13:R46.
34. Burstein HJ, Harris LN, Gelman R, Lester SC, Nunes RA, Kaelin CM, et al. Preoperative therapy with trastuzumab and paclitaxel followed by sequential adjuvant doxorubicin/cyclophosphamide for HER2 overexpressing stage II or III breast cancer: a pilot study. J Clin Oncol 2003;21:46–53.
35. Gennari R, Menard S, Fagnoni F, Ponchio L, Scelsi M, Tagliabue E, et al. Pilot study of the mechanism of action of preoperative trastuzumab in patients with primary operable breast tumors overexpressing HER2. Clin Cancer Res 2004;10:5650–5.
36. Phillips GDL, Li G, Dugger DL, Crocker LM, Parsons KL, Mai E, et al. Targeting HER2-positive breast cancer with trastuzumab-DM1, an antibody-cytotoxic drug conjugate. Cancer Res 2008;68:9280–90.
37. Doronina SO, Mendelsohn BA, Bovee TD, Cerveny CG, Alley SC, Meyer DL, et al. Enhanced activity of monomethylauristatin F through monoclonal antibody delivery: effects of linker technology on efficacy and toxicity. Bioconjug Chem 2006;17:114–24.
38. Hanson PI, Cashikar A. Multivesicular body morphogenesis. Annu Rev Cell Dev Biol 2012;28:337–62.
39. Maxfield FR, McGraw TE. Endocytic recycling. Nat Rev Mol Cell Biol 2004;5:121–32.
40. Rotin D, Kumar S. Physiological functions of the HECT family of ubiquitin ligases. Nat Rev Mol Cell Biol 2009;10:398–409.
41. Li X, Zhou Q, Sunkara M, Kutys ML, Wu Z, Rychahou P, et al. Ubiquitylation of phosphatidylinositol 4-phosphate 5-kinase type I gamma by HECTD1 regulates focal adhesion dynamics and cell migration. J Cell Sci 2013;126:2617–28.
42. Huang X, Gao L, Wang S, McManaman JL, Thor AD, Yang X, et al. Heterotrimerization of the growth factor receptors erbB2, erbB3, and insulin-like growth factor-i receptor in breast cancer cells resistant to herceptin. Cancer Res 2010;70:1204–14.
43. Lu Y, Zi X, Zhao Y, Mascarenhas D, Pollak M. Insulin-like growth factor-I receptor signaling and resistance to trastuzumab (Herceptin). J Natl Cancer Inst 2001;93:1852–7.
44. Ritter CA, Perez-Torres M, Rinehart C, Guix M, Dugger T, Engelman JA, et al. Human breast cancer cells selected for resistance to trastuzumab in vivo overexpress epidermal growth factor receptor and ErbB ligands and remain dependent on the ErbB receptor network. Clin Cancer Res 2007;13:4909–19.
45. Narayan M, Wilken JA, Harris LN, Baron AT, Kimbler KD, Maihle NJ. Trastuzumab-induced HER reprogramming in "resistant" breast carcinoma cells. Cancer Res 2009;69:2191–4.
46. Pohlmann PR, Mayer IA, Mernaugh R. Resistance to trastuzumab in breast cancer. Clin Cancer Res 2009;15:7479–91.
47. Kataoka Y, Mukohara T, Shimada H, Saijo N, Hirai M, Minami H. Association between gain-of-function mutations in PIK3CA and resistance to HER2-targeted agents in HER2-amplified breast cancer cell lines. Ann Oncol 2010;21:255–62.
48. Nagata Y, Lan KH, Zhou X, Tan M, Esteva FJ, Sahin AA, et al. PTEN activation contributes to tumor inhibition by trastuzumab, and loss of PTEN predicts trastuzumab resistance in patients. Cancer Cell 2004;6:117–27.